High-efficiency, low-speckle contrast white laser lighting via multi-stage scattering and photon recycling

Jifeng Liu (jifeng.liu@dartmouth.edu)
Dartmouth College https://orcid.org/0000-0003-4379-2928
Xiaoxin Wang
Dartmouth College
Charles Carver
Columbia University
Nicholas Shade
Dartmouth College https://orcid.org/0000-0002-9510-5627
Eric Fossum
Dartmouth College
Xia Zhou
Columbia University

Article

Keywords: laser diode lighting, multiple scattering, speckle contrast, direct color-mixing, phosphor-converted lighting

Posted Date: August 3rd, 2023

DOI: https://doi.org/10.21203/rs.3.rs-3182555/v1

Additional Declarations: (Not answered)

High-efficiency, low-speckle contrast white laser lighting via multi-stage scattering and photon recycling

Xiaoxin Wang,[1,*] Charles J. Carver,[2] Nicholas R. Shade,[1] Eric R. Fossum,[1] Xia Zhou,[2,] and Jifeng Liu[1,*]

[1] Thayer school of Engineering, Dartmouth College, 15 Thayer Drive, Hanover, NH 03755 USA
[2] Department of Electrical Engineering and Computer Science, Columbia University, Mudd Building, 500 W 120th St, New York, NY 10027, USA

***Corresponding Authors**

Xiaoxin Wang − Thayer School of Engineering, Dartmouth College, Cummings 230, 15 Thayer Drive, Hanover, New Hampshire 03755, United States. Email: Xiaoxin.Wang@dartmoth.edu ORCID: 0000-0002-8307-6507

Jifeng Liu − Thayer School of Engineering, Dartmouth College, ECSC 122,15 Thayer Drive, Hanover, New Hampshire 03755, United States; Email: jifeng.liu@dartmouth.edu Tel: 603-646-9885 ORCID: 0000-0003-4379-2928

Authors

Charles Carver − Email: cjc2306@columbia.edu ORCID: 0000-0002-6664-1893
Nicholas R. Shade − Email: Nicholas.R.Shade.TH@dartmouth.edu. ORCID: 0000-0002-9510-5627
Eric. R. Fossum− Email: Eric.R.Fossum@dartmouth.edu ORCID: 0000-0002-6232-0515
Xia Zhou: Email: xia@cs.columbia.edu ORCID: 0000-0002-2852-9024

Abstract:
Lighting consumes >10% of the global electricity. White laser lighting, utilizing either direct color mixing or phosphor-conversion, can potentially boost the efficiency well beyond existing light emitting diodes (LEDs) especially at high current density. Here we present a compact, universal packaging platform for both laser lighting schemes, which is simultaneously scalable to wavelength division multiplexing for visible light communication. Using commercially available laser diodes and optical components, low-speckle contrast ≤5% and uniform illumination is achieved by multi-stage scattering and photon recycling through a mixing rod and static diffusers in a truncated-pyramidal reflective cavity. We demonstrate a high luminous efficacy of 274 lm/W_o for phosphor-converted laser lighting and 150 lm/W_o for direct red-green-blue laser mixing, respectively, in reference to the input optical power. In the former case, the luminous efficacy achieved for practical lighting is even higher than most of the previous reports measured using integrating spheres. In the latter case of direct laser color mixing, to our best knowledge, this is the first time to achieve a luminous efficacy approaching their phosphor-conversion counterparts in a compact package applicable to practical lighting. With future improvement of blue laser diode efficiency and development of yellow/amber/orange laser diodes, we envision that this universal white laser package can potentially achieve a luminous efficacy >275 lm/W_e in reference to the input electrical power, ~1.5x higher than state-of-the-art LED lighting and exceeding the target of 249 lm/W_e for 2035.

Key words: laser diode lighting; multiple scattering; speckle contrast; direct color-mixing; phosphor-converted lighting;

Introduction

Lighting accounts for >10% of the global electricity consumption in 2022, increasing from 2021.[1,2] The deployment of efficient light-emitting diode (LED) lighting sources reduces the energy consumption by 75% with 25 times longer lifetime compared to the incandescent lighting, saving 500 TWh of energy per year.[2] Currently, the luminous efficacy of phosphor-converted LED (PC-LED) is 185 lm/W_e for cool white and 165 lm/W_e for warm white in reference to the input electrical power, and it is projected to reach the practical limit of 250 lm/W_e by 2050.[2]

However, LED efficiency is still limited by efficiency droop at high current densities, mainly due to the non-radiative Auger processes at high carrier densities in LED active regions.[3] The droop can be mitigated by utilizing laser diodes (LDs), in which the radiative recombination rate is greatly boosted once stimulated emission (lasing) becomes dominant, effectively overcoming Auger processes. Therefore, LDs can potentially offer high luminous flux at high efficiency. Another important driving force behind LD lighting is visible light communication (VLC), simultaneously providing lighting and high-speed wireless datalinks at >several Gb/s without band licensing issues or electromagnetic interference (EMI).[4]

Similar to LED lighting, the available architectures for LD-based light sources include phosphor conversion (PC) [5,6] and direct color-mixing (CM). [7,8] PC-LDs can achieve high color rendering index (CRI) and reduce the coherence-induced laser speckles by scattering the laser beam.[9, 10] It has been applied to automobile lamplights, featuring 1000 times brightness with 30% energy saving compared to their LED counterparts.[11] Just as PC-LEDs, the major drawback of PC-LDs is the energy loss due to the quantum efficiency of phosphors and the inherent Stokes-shift of the down-conversion, from the high-energy excitation laser photons to the low-energy phosphor-emitted ones. CM-LD lighting can potentially surpass PC-LD and achieve a high luminous efficacy of radiation (LER) of 350 lm/W and high color performance (CRI ~ 85) by carefully choosing the constituent laser line spectra in Blue-Green-Yellow-Orange (BGYO) scheme. [7,8,12] Currently, the limited efficiency of green and yellow lasers are the bottleneck. On the other hand, the advances in high-efficiency lasers (particularly yellow/amber/orange LDs) and sophisticated design of optical, electronic and heat-sink systems may speed up the development of CM-LD white lighting. However, for both schemes there is a lack of thorough evaluation of irradiation performances to achieve simultaneously speckle suppression, [13,14,15] color mixing, [16,17] uniform illumination,[18] high LER, and high CRI in a compact laser luminaire package. Furthermore, the solid-state lighting community and VLC community focus on different figures of merit, lacking synergy to achieve both high-performance white lighting and high communication rate. For example, dichroic mirrors are commonly used in laser mixing for VLC, [18,19,20] yet they are not directly applicable to lighting due to the large footprint and insufficient speckle removal.

In this paper, we demonstrate low-speckle, high-efficiency white LD lighting via multi-stage mixing and scattering in a reflective cavity using commercially available optical components that are highly scalable to practical applications. Using an acrylic mixing rod (light guide) and diffusers assists the process of color mixing and speckle removal. A truncated-pyramid reflective cavity recycles a large fraction of the back-scattered photons to enhance the output efficiency and fold the beam profile several times to improve the irradiance uniformity via superposition. This way, the adequate de-coherence of laser beams also addresses the eye safety concern. The key design parameters of LD luminaire performance are systematically investigated. After balancing these factors, we experimentally demonstrate RGB CM-LD lighting with a light extraction efficiency $\geq$ 60%, a correlated color temperature (CCT) of 4500 K, a speckle contrast $\leq$ 5%, and a luminous efficacy of 150 lm/W_o with respect to the input laser power. To our best knowledge, this

is the first experimental demonstration of a CM-LD lighting luminous efficacy comparable to their PC-LD counterparts (100-200 lm/W_o) in a compact package applicable to practical lighting. Built upon CM-LEDs, future development of amber/orange LDs can potentially achieve a high luminous efficacy >300 lm/W_e in reference to the input electrical power. Furthermore, this LD luminaire package is universal for both CM-LD and PC-LD lighting. A simple replacement of the output diffuser with a yellow phosphor plate achieved a high PC-LD lighting luminous efficacy up to ~300 lm/W_o in referenced to the input laser power and a CRI of ~90 in a practical lighting configuration, surpassing most of their peers measured using integrating spheres in previous literature. Future improvement of blue LD efficiency can potentially achieve a luminous efficacy >275 lm/W_e in reference to the input electrical power, ~1.5x higher than state-of-the-art LED lighting and exceeding the target of 249 lm/W_e for 2035. This package is simultaneously scalable to accommodate multiple LDs for wavelength division multiplexing (WDM) in VLC.

Results

Design and Modeling

Design Overview. The CM-LD lighting prototype consists of three LDs (RGB), an acrylic mixing rod, and two types of diffusers integrated into a truncated-pyramid reflective cavity, as shown in Fig. 1a. This configuration is scalable to 4 or more LD mixing for better CRI and/or WDM in VLC, as will be detailed in the **Discussion**, thanks to multiple scattering and reflection that effectively homogenize the output white light irrespective of the positions of the LDs. Details of the LD parameters are provided in Section 1 of the Supplemental Information.

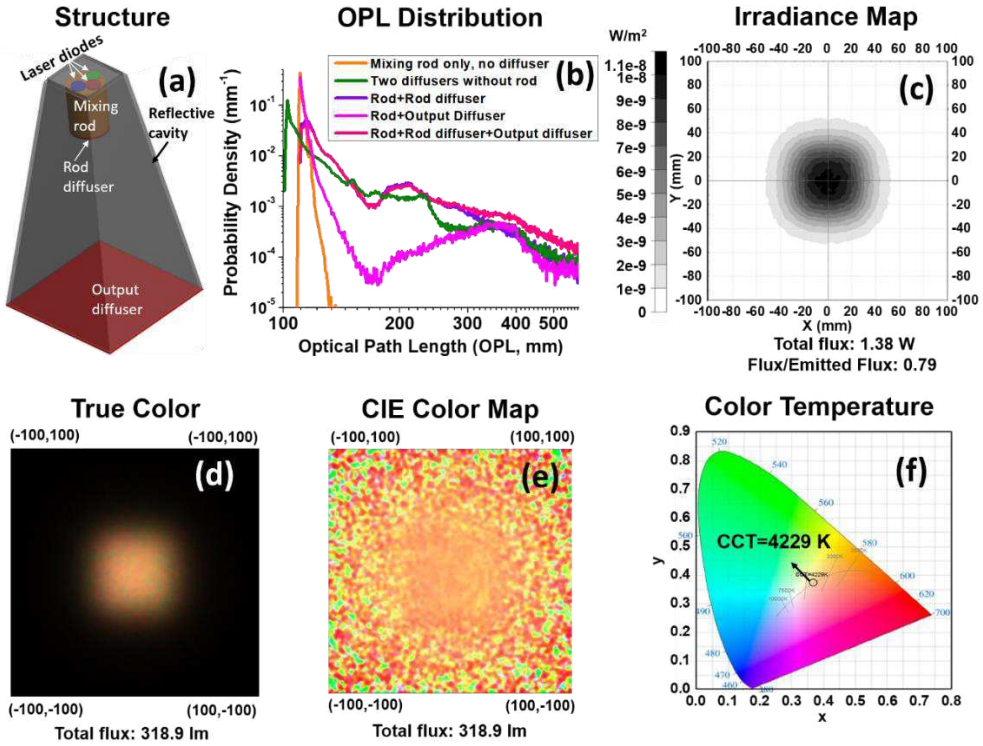

Fig. 1 (a) Schematics of the white laser package, comprising RGB laser diodes, a mixing rod, a truncated-pyramidal reflective cavity, and two types of diffusers (at the end of the mixing rod and the end of the reflective cavity, respectively). (b)-(f) show the ray-tracing modeling results for a 20 mm long rod inserted

into the 100-mm-high 8.5° reflective cavity (ideal reflectivity R=100%). The three laser power ratios are P_{R640}:P_{G520}:P_{B450}=1 W: 0.55 W: 0.2 W. A detection target is located 25 mm away from the output diffuser. (b) shows the optical path length (OPL) histogram for the complete package as well as other configurations to elucidate the impact of the components on the OPL distribution. For the completed package, (c) shows the corresponding irradiance distribution mapping; (d) shows the true color; (e) shows the Commission Internationale de l'Elcairage (CIE) color correlated temperature (CCT) distribution mapping, and (f) indicates that the CCT at the center of (e) is 4229 K.

The mixing rod has a diameter d=20 mm and a length L in the range of 10 ~ 80 mm. A truncated-pyramid shape is selected for the reflective cavity for good color-mixing and simplicity of fabrication, which has been investigated for laser projection imaging before. [14] To match the diameter of the mixing rod, the input port is chosen to be 20x20 mm^2. A reflective cap (20×20 mm^2) is used to secure the three LDs and seal the top of the reflective cavity. The sidewall tilt angle of the reflective cavity is an important parameter. If the tilting angle is too small (i.e., nearly vertical sidewall), the laser beams tend to be guided in the rod and trapped inside the cavity. If the tilt angle is too large, it might be hard to achieve uniform color mixing and white illumination via multiple reflections. Three types of reflective cavities are investigated to understand the trend, as listed in Table 1. The interior surfaces of the truncated pyramidal cavity and reflective cap have a specular reflectivity of either 100% (for modeling perfect mirrors, e.g. high refractive index contrast distributed Bragg reflectors (DBR)) or 95% (for modeling more commonly used metallic mirrors). Two 0.5 mm-thick diffusers attached to the bottom of the mixing rod are named rod diffusers, while the 0.5 mm-thick diffuser sealed at the bottom of the reflective cavity is called output diffuser. They are modeled after DiffsTEK^{TM} diffusers D6060 and D3030 [21] (Fusion Optix, Inc.) to guide experimental prototyping, as detailed in Materials and Methods.

Table 1. Geometrical dimensions of three types of truncated-pyramid reflective cavities

Name	Sidewall Tilt Angle	Height of the Cavity	Size of the Output Opening
8.5° cavity 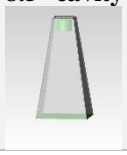	8.5°	100 mm	50×50 mm^2
19.3° cavity 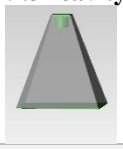	19.3°	100 mm	90×90 mm^2
Extended Cavity 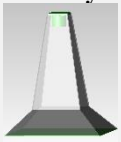	Top part: 8.5° Bottom part: 19.3°	Top part: 100 mm Bottom part: 25 mm	67.4×67.4 mm^2

Modeling Results. Ray-tracing simulation results of a typical CM-LD configuration are shown in Fig. 1b-e for an 8.5° reflective cavity (as described in Table 1) with a 20 mm-long mixing rod, two rod diffusers, and one output diffuser. The specular reflectivity of the interior surfaces is assumed wavelength-independent at R=100%. The optical power ratio of RGB lasers are P_{R640}:P_{G520}:P_{B460}=1 W: 0.55 W: 0.2 W to best approximate the desired warm white color. A power-

detection target is located at 25 mm away from the output diffuser. Firstly, the RGB laser beams are coupled and guided in the short mixing rod. Then the bulk scattering from the rod diffusers redirect the light to the highly reflective interior surfaces of the truncated-pyramidal cavity. Multiple internal reflections fold the beam profiles several times, leading to a good homogenization and color mixing. The output diffuser allows further bulk scattering and forward transmission of a large fraction of the CM-LD white light. The multi-stage scattering and mixing within the reflector cavity helps to recycle photons, suppress laser speckles and achieve adequate color mixing. This is quantitatively detailed by the simulated histograms of optical path length (OPL) of photons in the cavity (Fig. 1b). With mixing rod alone, the optical path length is increased slightly beyond 100 mm (cavity height) due to waveguiding in the rod, but the OPL distribution is too narrow to induce decoherence for speckle removal. Incorporating diffusers can greatly broaden the distribution of OPL due to multiple scattering and reflection. The data for rod+rod diffuser vs. rod+output diffuser clearly show a dramatically broadened OPL distribution compared to mixing rod only. This comparison also indicates that the first resonant feature at OPL ~200 mm is induced by the rod diffuser, while the second one at OPL~400 mm is induced by the output diffuser. When both diffusers are integrated with the mixing rod, we achieved a mean OPL of 193 mm (i.e. ~2x the physical length of the cavity) with a very large standard deviation of 127 mm thanks to the multiple scattering induced by the diffusers. The large standard deviation of the OPL directly transfers to a broad distribution of phases for the scattered laser light, effectively leading to decoherence and speckle pattern removal.

From the irradiance and color mappings in Fig. 1c-f, RGB lasers are mixed well in the central regime of ~60 × 60 mm^2. The irradiance (Fig. 1c), true color (Fig. 1d) and CCT (Fig. 1e) all show good uniformity, and the CCT of ~4200 K indicates good approximation of natural light. The light extraction efficiency is η_{ex}=79%, defined as the ratio of output optical power of 1.38 W to the input laser power of 1.75 W. The LER and luminous efficacy in reference to the input optical power (LEO), as defined in Materials and Methods, are 231 lm/W_o and 182 lm/W_o, respectively,.

Table 2 Modelled Irradiance, true color, and CIE color temperature maps for different mixing rod and diffuser configurations. The rod is 20 mm long and the 8.5° cavity is 100 mm high with 100% reflectivity.

	Rod Only	Output Diffuser Only	Rod + Output diffuser	Both Diffusers Only (No Rod)	Rod + Rod Diffuser	Complete Package
Irradiance Map	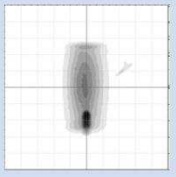	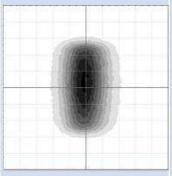	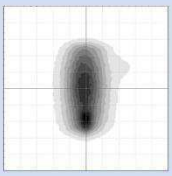	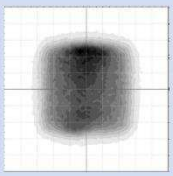	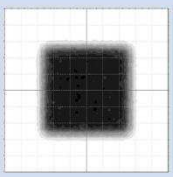	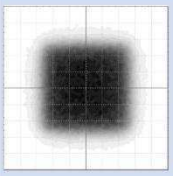
Real Color	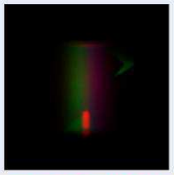		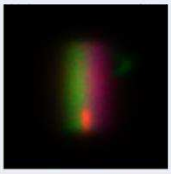		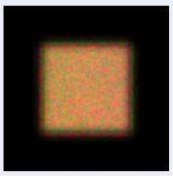	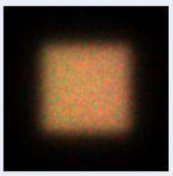
CIE Color Map	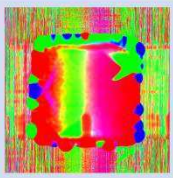	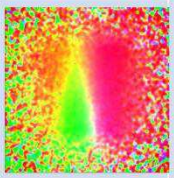	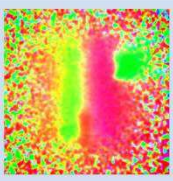	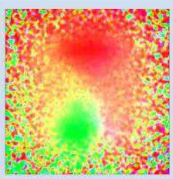	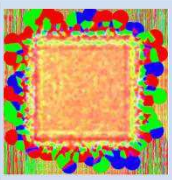	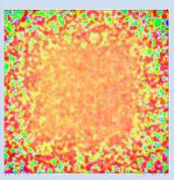

To elucidate the contribution of each component to the color mixing, Table 2 further shows the modeled color mixing results under different mixing rod and diffuser configurations. With the mixing rod only, output diffuser only or rod+output diffuser (see the first 3 columns), the mixing is insufficient such that the output pattern is rectangular since the ellipsoidal far field patterns from the edge emitting green and blue lasers (see Figs. 2b-c) cannot be fully overcome. With both output diffuser and rod diffuser but no mixing rod (column 4), the output pattern looks more square in shape yet the color mixing is still poor. With rod+rod diffuser (column 5), the mixing is almost satisfactory except for some edge effect that can be seen clearly from the CIE color temperature map in the last row. This is consistent with the OPL histogram shown in Fig. 1b, indicating that rod+rod diffuser almost achieves the same OPL distribution as the completed package. Finally, further adding the output diffuser smoothed out the edges due to further increase in the standard deviation of OPL.

Interestingly and counterintuitively, when using an 8.5° conical cavity with a circular cross-section and keeping other setup parameters the same, our simulations reveal discrete color regions on the detection plane (Supplemental Information Fig. S1). This counterintuitive result is because conical cavity tends to maintain the original axial distribution of the input LD configuration. Since the RGB LDs are placed on 3 different locations rather than overlapping each other in the center, having a perfect rotational axial symmetry actually prevents effective laser mixing. As demonstrated in Fig. S1, the RGB light spots are separated similar to their LD configuration inside the conical cavity. Instead, the truncated pyramidal cavity with a square cross-section reduces the rotational symmetry, which is actually better for homogenizing LD sources at different locations due to multiple reflection. [14]

Table 3 further compares the normalized irradiance distribution mapping and the light extraction efficiency η_{ex} for the 3 types of reflective cavity design and mixing rod lengths. This is also complemented by Fig. S2 of the Supplemental Information to provide a basic guideline to select the cavity type, interior specular reflectivity and rod length in order to balance the trade-off between irradiance uniformity and η_{ex}. Overall, the CM-LD light is more uniformly distributed in the 8.5° cavity. Non-uniformity of irradiance is clearly observed in the 19.3° cavity because some light rays scattered from the rod bottom diffusers escape the cavity directly without taking part in multiple reflections off the interior surface. This issue worsens as the rod length exceeds half of the cavity height. The output light is more concentrated in a circular area similar to the rod cross-sections for L=60 mm and L=80 mm, indicating that a large percentage of rays only propagates in the mixing rod without hitting the inner surface of the reflective cavity. Therefore, in order to balance the light extraction efficiency η_{ex} (favoring larger sidewall tilt angle) and mixing uniformity (favoring smaller sidewall tilt angle), the aforementioned extended cavity integrating 8.5° and 19.3° sections is modeled in the last two rows of Table 3. As expected, it generally achieves a higher light extraction efficiency than the 8.5º cavity and much better irradiance uniformity than the 19.3° cavity at the same mixing rod length and interior surface reflectivity. The light extraction efficiency of the extended cavity reaches η_{ex}~82% for R=100% and ~72% for R=95%, respectively, suggesting that the laser beams reflects off the inner surface 2.54 times on average in the extended cavity (i.e. $(0.95)^{2.54}$=0.72/0.82). We also noted that for perfectly reflective interior surface (R=100%), η_{ex} decreases with increasing mixing rod length due to light trapping inside the rod. For R=95%, on the other hand, increasing mixing rod lengths enhances η_{ex} by a few percent due to longer waveguiding in the mixing rod and less interior surface reflection losses, yet it also adversely affects the output uniformity. In our future work, we will further optimize the geometrical pairing of the mixing rod and the reflective cavity to better balance the color mixing

uniformity and light extraction efficiency. For facile experimental verification of the modeling, though, in this work we will focus on the three types of simple cavity structures shown in Table 1.

Table 3 Normalized irradiance distribution mapping and extraction efficiency vs. mixing rod length in the reflective pyramidal cavities with different tilt angles and different interior specular reflectivity.

Cavity	Rod Length (mm)					
	10	20	40	60	80	
8.5° cavity R=100%	η_{ex} =79.7%	η_{ex} =79.1%	η_{ex} =78.1%	η_{ex} =77.4%	η_{ex} =76.4%	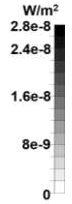
19.3° cavity R=100%	η_{ex} =81.6 %	η_{ex} =81.3 %	η_{ex} =81.3%	η_{ex} =81.0%	η_{ex} =80.6%	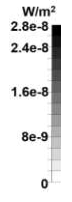
Extended cavity R=100%	η_{ex} =81.5%	η_{ex} =80.8%	η_{ex} =80.3%	η_{ex} =79.9%	η_{ex} =79.4 %	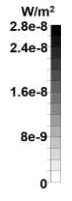
Extended cavity R=95%	η_{ex} =71.5%	η_{ex} =71.1 %	η_{ex} =71.5%	η_{ex} =71.9%	η_{ex} =72.9%	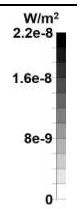

Experimental results

Prototype white laser mixing cavities based on the design and modeling in the previous section are constructed using off-the-shelf commercial products. As examples, photos of the 8.5° cavity and extended cavity packaging are shown in Fig. S3 and detailed in Section 4 of the Supplemental Information.

Baseline LD speckle and color mixing characterization. We first characterize the speckles and color mixing of the bare RGB LDs as a baseline, i.e. without the mixing rod or reflective cavity. The laser beams shine on a letter-sized print paper screen at a distance of 30 cm. Figs. 2a-d represent the images of discrete red, green, blue laser beams and RGB mixed light (with the 3 LDs mounted as shown in Fig. S3a), respectively. The measurement of speckle contrast K_s is described in Materials and Methods, and the K_s values are calculated to be 8.3%, 11.4% and 10.3% for the

red, green and blue LDs in Figs. 2a-c, respectively. Fig. 2d further shows very poor color mixing without the white laser pacakging.

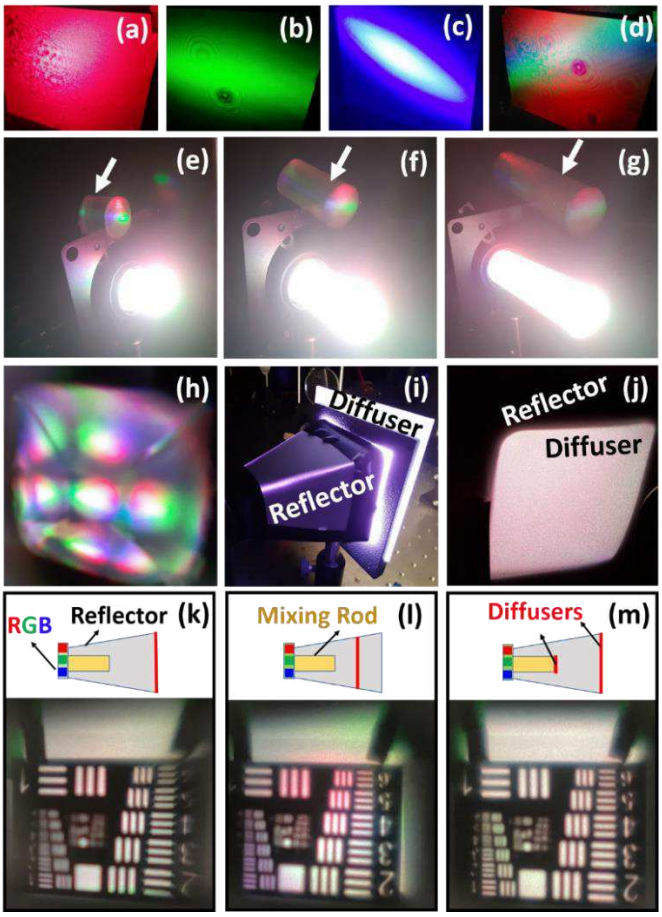

Fig.2 Speckle images of (a) the red LD (110 mW at λ=670 nm), K_s=8.3%; (b) the green LD (17 mW at λ=520 nm, K_s=11.4% (c) the blue LD (15 mW at λ=450 nm), K_s=10.3%; (d) mixed light using bare LDs shown in (a)-(c). Images of RGB laser beams guided in mixing rods are shown for (e) 10 mm-long mixing rod with pristine lateral surface, (f) 20 mm-long rod with mechanically roughed lateral surfaces and two rod diffusers DiffsTEK™ D6060 [21], and (g) 55 mm-long rod with mechanically roughed lateral surface and two D6060 rod diffusers. The white arrows indicate the images taken through neutral density filters. (h) Multiple images of the mixing rod formed inside the 8.5° cavity, showing multiple reflections at interior surfaces of the cavity. (i) Image of the 8.5° cavity with the 20 mm-long mixing rod in (f). (j) An image of uniformly mixed light coming through the output diffuser D6060 of the 8.5° cavity in (i), with an interior surface reflectivity of R=95%. Images of the USAF resolution test chart in the transmission mode from the outupt port of the CM-LD 8.5° cavity are shown for various D6060 diffuser configurations: (k) only one output diffuser, (l) only one layer of diffuser placed inside the cavity, 20 mm from the end of the mixing rod, and (m) both rod diffuser and output diffuser. The insets in (l-m) illustrate the diffuser configurations.

The effect of the mixing rod. Figs. 2e-g reveal the guiding and mixing of RGB laser beams by the acrylic rod and rod diffusers, without the cavity and output diffuser. The lengths and surface conditions of the mixing rods are given in the captions. The laser beams appear very bright and white because the intensity is strong enough to saturate the CMOS camera. Neutral density filters are then used to attenuate the light entering the camera, and the corresponding images are indicated with white arrows in each figure. The three laser beams are well guided in the mixing rod. The

increase in the rod length and the use of bottom diffusers facilitate the color-mixing, blurring the three primary colors as shown in Fig. 2f-g, in contrast to Fig. 2e. When the mixing rod is inserted into the 8.5° reflective cavity, multiple internal reflections from the inner surface of the cavity is clearly visualized through multiple reflection images of the mixing rod (Fig. 2h).

The impact of diffuser configurations. When an output diffuser is added to the cavity in Fig. 2h, the strong scattering at the exit port of the cavity (Fig. 2i) further reduces the spatial coherence of the incident beams, enhancing the color-mixing and speckle suppression, as shown in the image taken with an angle of 45° from the output diffuser (Fig. 2j). Consistent with our modeling shown in Fig 1b and Table 2, the position and number of diffusers affect the CM-LD lighting uniformity and speckle contrast significantly. The insets in Fig. 2k-m illustrate various diffuser configurations. The emission from the output port of the cavity is directed onto a U.S. Air Force (USAF) resolution test chart and subsequently imaged onto a CMOS camera. The corresponding images of the USAF resolution test chart in the transmission mode are shown in Fig. 2k-m. The clearly resolved patterns indicate that the speckles are effectively suppressed with an output diffuser attached to the end of the cavity. The K_s values corresponding to Figs. 2k-m are 6.8%, 7.3% and 5.0%, respectively, showing that the combination of a rod diffuser with an output diffuser delivers lower speckle contrast and more uniform color mixing, consistent with the modeling shown in Table 2.

Performance of Extended Cavities compared to 8.5º cavities. Since our modeling indicates that the extended cavity offers a good balance between color/irradiance uniformity and light extraction efficiency (Table 3), it is interesting to compare the performance of extended cavities structures with their 8.5º counterparts experimentally.

Illumination uniformity. The experimental measurement of illumination uniformity is decribed in Materials and Methods, where the average deviation (AD) of luminous intensity (lux) across 48 regions on a letter-sized paper is used to quantity the nonuniformity. A lower AD is preferred for more uniform lighting. Our target is reaching similar or lower AD values than LED lighting, i.e. in the range of 10%~18%. [22] Fig. 3 summarize the AD values measured for the 8.5º cavity vs. the extended cavity, with different mixing rod lengths and surface conditions as well as diffuser types and configurations. Two type of DiffsTEK™ diffusers [21] are compared: D6060 with transmittance of 80% and angular distibution of 60°, and D3030 with transmittance of 90% and an angular distribution of 30°. Their transmittance spectra can be found later in Fig. 5c. For the 8.5° cavity packaing with a 55 mm long rod (Fig. 3a), the lowest AD of 6.0% is achieved when using two rod diffusers D6060, one output diffuser D6060 (abbreviated as D6060(2)/D6060) and a surface-roughened rod. It represents 45% reduction in AD compared to the case of D6060(2)/D6060 and a smooth rod in Fig. 3(a). More scattering from the roughened rod surface is beneficial to homegenization[14] and color-mixing, in agreement with observations in Fig. 2e-g. On the other hand, there is a trade-off between the light extraction efficiency η_{ex} and irradiance uniformity for different diffusers. When utilizing D3030 diffusers with strong forward scattering and high transmittance, η_{ex} is enhanced (shown later in Fig. 4a) at the cost of the uniformity. The combination of two D3030 rod diffusers and one output diffusers (D3030(2)/D3030) has an AD of ~13.5%, larger than that of D6060(2)/D3030 (8.7%) and D6060(2)/D6060 (6.0%) in a 8.5° cavity. That said, this AD value is still desirably comparable to that of LED lighting.

Among the mixing rod lengths investigated for the extended cavity, the case of L=55 mm offers the minium AD of 12.5% and 15.5% for the diffuser combinations of D6060(2)/D3030 and D3030(2)/D3030, respectivly (Fig. 3b). These AD values are comparably to that of LED lighting. The extended cavity configuration introduces an additional 2-4 % in AD as compared with the 8.5°

cavity for the same mixing rod length, which is consistent with the irradiance mappings in Table 3. This is a trade-off in enhancing light extraction efficiency η_{ex}, as mentioned earlier.

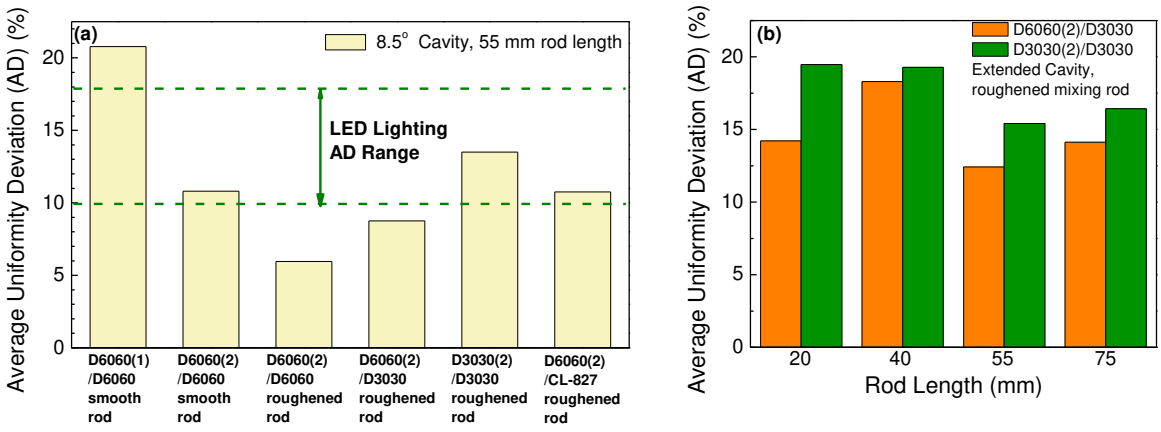

Fig. 3 Average uniformity deviation measured in two different cavity configurations, (a) 8.5° cavity, 55 mm long rod with different rod lateral surfaces and diffuser combinations, (b) extended cavity, different rod lengths and diffuser combinations.

It is also interesting to note that the commercial yellow phosphor plate CL-827 acts as an output diffuser to get a similar uniformity. An AD value of 10.8% is achieved for D6060(2)/CL-827 in Fig. 3a. Therefore, this CM-LD packaging is readily applicable to PC-LD lighting by simply replacing the output diffuser with a phosphor plate without degrading the uniformity. The irradiance uniformity of CM-LD and PC-LD lighting for the 8.5° cavity and extended cavity shown in Fig. 3 is comparable to LED-based illuminators.[22]

Light Extraction Efficiency η_{ex}. We then verify that the light extraction efficiency η_{ex} is notably enhanced in the extended cavity structure, as theoretically predicted in Table 3 and experimentally demonstrated in Fig. 4. The use of high-transmission D3030 diffusers renders higher η_{ex} with larger standard deviation compared to D6060. The standard deviation of η_{ex} is consistent with the trend of AD values discussed earlier. The higher the η_{ex}, the larger standard deviation and uniformity deviation, confirming the trade-off between extraction efficiency and irradiance uniformity. Due to the optical leakage loss at the seals of the 8.5° cavity, the measured maximal η_{ex} (~40%) in Fig. 4a is less than the simulated value (~68%) predicted in Fig. S2. On the other hand, measured η_{ex} of the 8.5° cavity (R=95%) is slightly increased with the increment in the rod length L, indeed in agreement with the trend of the simulated η_{ex} as a function of the rod length in Fig. S2(a).

By comparison, the η_{ex} values of the extended cavity packaging with minimal leakage loss are much closer to the simulated value of ~70% for R=95% (the last row in Table 3). The maximum η_{ex} is 57.8%±12.4% for the configuration of 75 mm long rod and D3030(2)/D3030 diffusers, while reducing the rod length to 40 nm achieved a similar efficiency η_{ex} of 57.1% ±6.7% at a much smaller standard deviation. These η_{ex} values are comparable to the packaging efficiency of CM-LED lighting (~60%).[16] The discrepancy between measured η_{ex} and simulated η_{ex} is due to the overestimated forward scattering parameters in the ray-tracing simulations compared to the actual diffuser performance, especially for D6060. One compelling evidence is that the discrepancy decreases from 31% to 15% when replacing three D6060 diffusers by three D3030 diffusers with higher transmission in the case of L=40 mm. More details are presented in Fig. S2(b) and S2(c) of the Supplemental Information.

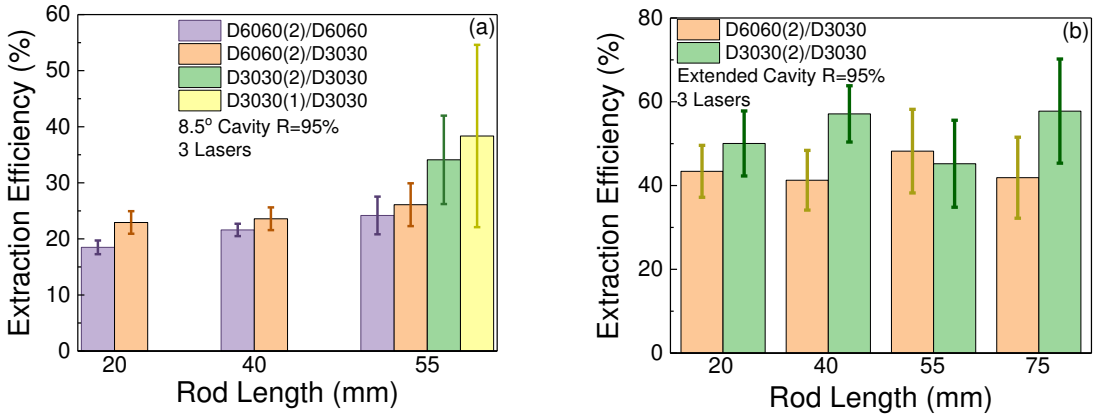

Fig. 4 Comparison of measured extraction efficiency (η_{ex}) as a function of the rod length L in various configurations, (a) 8.5° cavity, four types of diffuser combinations and (b) extended cavity, two types of diffuser combinations.

Lighting Quality Characteristics. More characteristics of CM-LD lighting in the 8.5° cavity and the extended cavity are shown in Fig. 5 and Fig. 6, respectively. After carefully choosing the electrical currents of the RGB lasers, the CCT of the mixed light is 6100 K with the 8.5° cavity (20 mm rod and D6060(2)/D6060 diffusers) in Fig. 5(a). Fig. 5(b) shows the distance-dependent CCT mapping (blue squares) and color uniformity mapping (red dots) at a distance of 10 cm from the output diffuser. CCT values are constant as a function of distance in the range of 10-30 cm, and the color uniformity is 6200K+/-500 K at a distance of 10 cm as mapped in an area of 10 cm x 10 cm. The inset of Fig. 5a is an image of the USAF resolution test chart and the speckle constrast is K_s=3.8%, confirming that an additional rod diffuser D6060 can further suppress the speckles, in comparistion with K_s=5.0% for the diffuser combination D6060(1)/D6060 in Fig. 2m.

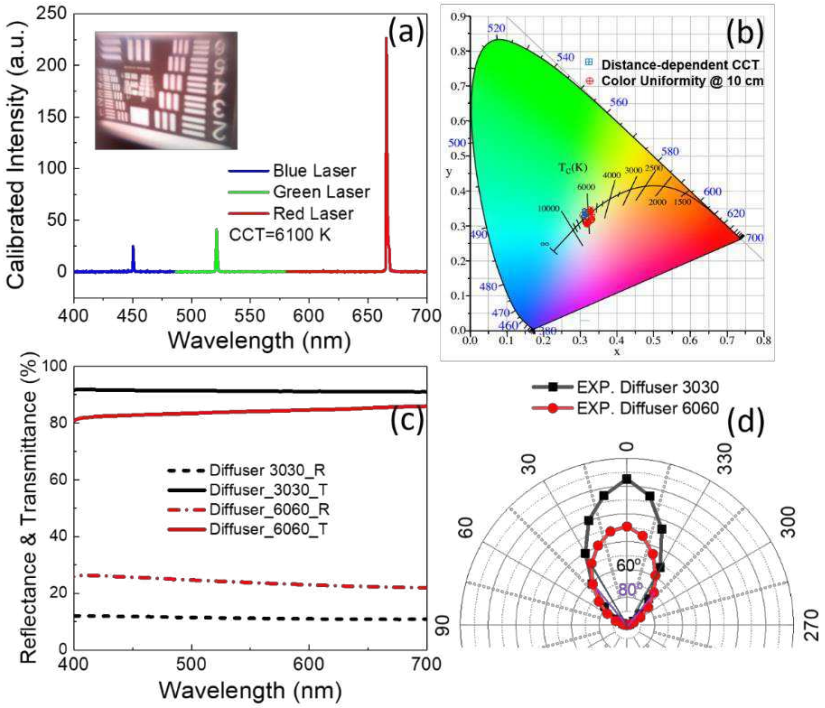

Fig. 5 (a) Irradiance spectrum from the 8.5° cavity packaging consisting of a 20 mm long rod and D6060(2)/ D6060 diffusers. The inset is the image of the USAF resolution test. (b) Distance-dependent CCT mapping (blue squares) in the range of 10-30 cm and color uniformity mapping (red dots) in an area of 10 x10 cm^2 at a distance of 10 cm from the output diffuser. (c) Reflectance and transmittance spectra of diffuser D3030 and diffuser D6060 measured with an integrated sphere. (d) Comparison of measured angular distribution of the irradiance with the output diffuser D3030 and D6060.

Diffuser D3030 is also used to replace D6060 to evaluate the influence of the output diffuser on the lighting performance. The transmittance and reflectrance spectra of output diffuser D6060 and D3030 measured with an integrating sphere are shown in Fig. 5c, which are insensitive to the wavelength. Therefore, the choice of the output diffuser D6060 or D3030 has a miminal impact on the output CCT, but it affects the output intensity and angular distribution. As shown in Fig. 5(d), the full width half maximum (FWHM) of the measured angular distribution is 60° and 80° for output diffusers D3030 and D6060, respectively. Due to the high transmittance of diffuser D3030, the maximum output power after the output diffuser D3030 at the forward direction of 0° is 1.4 times that of the diffuser D6060. However, the illumination uniformity is degraded slightly with the output diffuser D3030 due to a smaller fraction of photons undergoing multiple-scattering and reflection in the cavity, referring to Fig. 3.

For the extended cavity, Fig. 6a shows an image of irradiance taken at 45° from the output diffuser. While the color mixing is effective in the central region, the sharp transition from the tilt angle of 8.5° to 19.3° leads to some edge effect, where green or red lines can be observed near the cavity exit edge. Hence, the extended cavity is required to be refined with a gradual tranisition structure to smear out the edge effect in the future work. The patterns on the USAF resolution target is clearly seen in Fig. 6b, and the speckle contrast is measured to be 4.3% with an integration time of 30 ms, close to the human speckle perception threshold (~4%).[23] Furthermore, Fig. 6c shows that the simulated normalized angular distribution of irradiance for various rod lengths agrees very well with the measured angular distribution. The FWHM of the angular irraidance distribution in L=20 mm, L=40 mm and L=75 mm cases are 53°, 62°, 75°, respectively. Clearly, the increment in the rod length increases the angular distribution in Fig. 6c, as the irradiance is focused in a smaller area for the longer rod in the extended cavity in Table 3. Therefore, these observations follow a law called conservation of étendue in that, by concentrating the area, the angular distribution of the irradiance will spread.

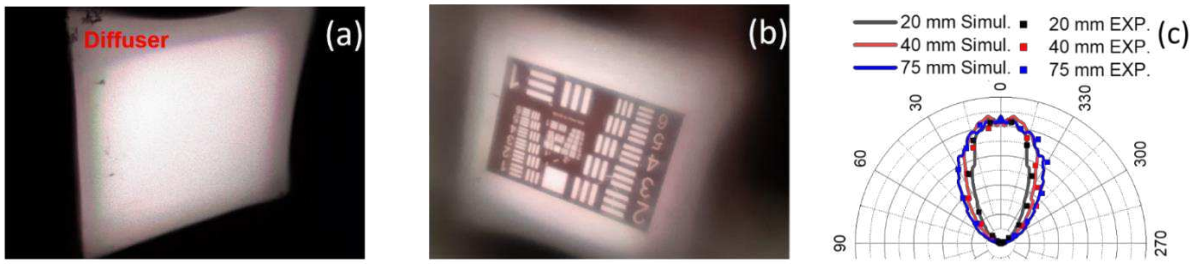

Fig. 6 (a) Image of irradiance taken at 45° from the output diffuser of the extended cavity. (b) Image of the USAF resolution test chart. The mixing rod length is 40 mm and diffuser combination is D6060(2)/D3030 in (a) and(b). (c) Comparison of measured and simulated normalized irradiance angular distribution of the irradiance with various rod lengths. The diffuser combination is D3030(2)/D3030 in the experimental setup.

Overall performance summary of the reflective cavity CM-LDs will be presented and discussed later in Discussion (Table 4), together with their PC-LDs counterparts, for comparison

with previous work in literature. Currently, CM-LDs are mainly limited by a low CRI~10 due to the lack of efficient amber/orange lasers to better match the luminosity function of photopic vision.

Reflective Cavity for PC-LD Lighting. Considering most PC-LED lights demonstrate a CRI Ra of 80 to 90, the PC-LD configurations may offer high color quality white lighting using available LDs (i.e. without efficient amber/orange ones). A simple replacement of the output diffuser in the reflective cavity packaging with a yellow phosphor place can convert the CM-LD configuration to the PC-LD configuration. A common issue of existing PC-LD packaging is that the transmitted blue laser light is focused with a small divergent angle, while yellow phosphor emission is scattered isotropically in all directions. The mismatch in the spatial intensity distribution between blue laser light and yellow light may result in poor angular color uniformity in the PC-LD lighting. [10, 24] Notably, the proposed reflective cavity PC-LD packaging can effectively address the angular color uniformity issue by homogenizing the blue laser beam and engineering the laser irradiance distribution using the mixing rod and diffusers. The phosphor plate at the cavity exit is then uniformly excited by blue laser light for better color mixing. The homogenization of blue excitation laser beams can also minimize the thermal quenching effect and damage of the phosphor converters. In addition, the reflective cavity can recycle the back-scattered photons to enhance the overall output flux and efficacy.

A typical PC-LD lighting configuration and its illumination characteristics are shown in Fig. 7 for an 8.5° cavity. The entire area of 6×6 cm^2 is uniformly illuminated in Fig. 7a. The normalized spectrum in Fig. 7b consists of a sharp blue excitation laser line and a broad phosphor luminescence. The measured angular irradiance distribution of the PC-LD agrees well with the Lambertian distribution, as shown in Fig. 7c. A CRI Ra of 86 is achieved with the PC-LD configuration. Other implemented PC-LD configurations and illumination performances are listed in Table 4 in the Discussion section, which will be discussed next.

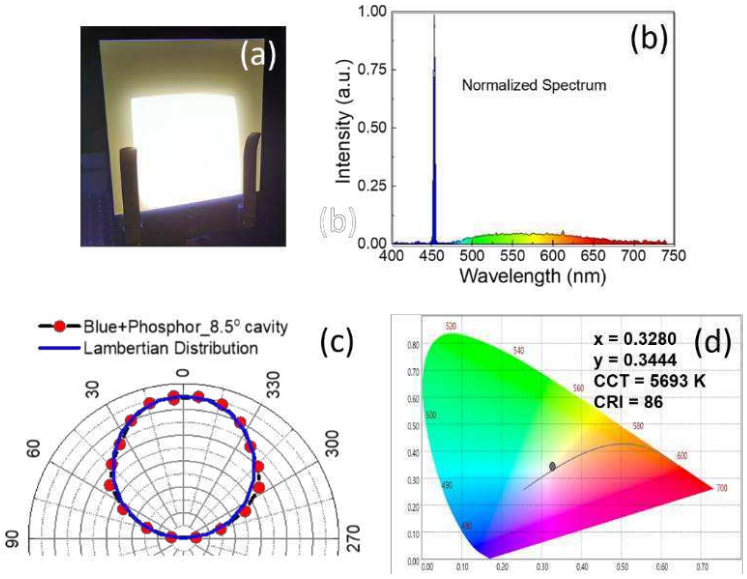

Fig. 7 White light illumination from a PC-LD using a 20 mm mixing rod and two D6060 rod diffusers in a 8.5° cavity. (a) An image of PC-LD white light illumination, (b) normalized white light spectrum consisting of the blue excitation laser line and broad phosphor luminescence, (c) measured angular distribution of the PC-LD white light irradiance, in good agreement with the Lambertian distribution, and (d) the corresponding CIE chromaticity showing a CCT of 5693 K.

Discussions

Table 4 summarizes the white light illumination performance of the experimentally implemented reflective cavity CM-LD and PC-LD white light sources in cool white (4000-5000 K) and daylight (5000-6000 K) color temperature ranges. In principle, LER of four lasers with yellow LD can be as high as 330 lm/W,[7, 8] so the LEO could be as high as 200 lm/W_o with CRI >85 using our existing extended cavity prototype (with a light extraction efficiency of η_{ex}~60%). Using more perfect DBR reflectors in the interior, η_{ex}~80% could be achieved based on Table 3, and the LEO can potentially reach >260 lm/W_o. However, due to the lack of efficient electrically pumped amber/orange LDs, in our prototype incorporating a deep red LD (λ_{peak}=670 nm) the highest LEO is ~110 lm/W_o with a CRI Ra of 30. Using a shorter wavelength red laser (λ_{peak} =640 nm) increases the LEO to 150 lm/W_o, yet degrades CRI to 10. Hence, similar to CM-LED lighting, there is a trade-off between efficacy and color quality. [2] A CRI R_a >80 is required for white lighting in most applications. Therefore, future development of high efficiency amber/orange lasers will greatly help to enhance both the efficacy and CRI of CM-LD lighting.

For the PC-LD package, the LEO is greatly improved from 113.5 lm/W_o for the 8.5° cavity to >208.3 lm/W_o using the extended cavity due to a large improvement in η_{ex} by ~2x with other configurations being identical. The highest luminous efficacy reaches as high as 274±47 lm/W_o when using two D3030 diffusers at the rod bottom. The standard deviation here reflects an average uniformity deviation of 17%, still comparable to white LED lighting. [16] For all the investigated PC-LD configurations, we achieve a speckle contrast $K_s \leq 4\%$ and a CRI Ra ≥ 85, and CCT varies between 5000 K~6000 K. Therefore, the packaging scheme proposed in this work has been demonstrated as a universal platform for both CM-LD lighting and PC-LD lighting.

Table 4 Summary of implemented configurations and measured illumination performance of CM-LD and PC-LD light sources in cool white and daylight color temperature ranges

Reflective Cavity	Type	Lasers (nm)	Rod Length (mm)	Diffusers (rod/output)	LEO (lm/W_o)	CCT (K)	CRI Ra	K_s* (%)
Extended (R=95%)	CM-LD	670/520/450	40	D3030(2)/D3030	110±13	7258	32	4.8
Extended (R=95%)	CM-LD	640/520/450	40	D6060(2)/D3030	125±20	4715	11	4.3
Extended (R=95%)	CM-LD	640/520/450	40	D3030(2)/D3030	153±25	4506	12	5.2
Extended (R=95%)	CM-LD **(4 LDs)**	670/640/520 /450	40	D3030(2)/D3030	93±10	5600	<10	4.8
8.5° (R=95%)	PC-LD	450	20	D6060(2)/CL-827	114±3	5693	86	3.0
Extended (R=95%)	PC-LD	450	20	D6060(2)/CL-827	208±6	4985	85	3.9
Extended (R=95%)	PC-LD	450	40	D6060(2)/CL-827	184±18	5304	86	3.7
Extended (R=95%)	PC-LD	450	40	D3030(2)/CL-827	245±26	5397	88	4.4
Extended (R=95%)	PC-LD	450	80	D3030(2)/CL-827	274±47	5235	86	4.1

*Speckle contrast is measured with an integration time of 30 ms.

Fig. 8 further compares the reported luminous efficacy of white LD lighting over the past decade. Most of the references are based on PC-LD white light. [6] The measurements are commonly

carried out on a blue laser chip and a phosphor plate in an integrating sphere, some incorporating specially fabricated phosphors and/or aspherical lenses, which are not directly applicable to practical white light illumination. The improvement in the luminous efficacy has mainly been contributed by the development of phosphor materials and fabrication techniques. In contrast, our extended cavity PC-LD light source is directly applicable to practical lighting using off-the-shelf blue LD and phosphor plate, and it demonstrates a high luminous efficacy of 274±47 lm/W_o, higher than most of the reported LEO measured in an integrating sphere. The corresponding CCT of 5235 K, a high CRI Ra of 86, and a low speckle contrast of K_S=4.1% all satisfy the standards for practical lighting in cool white range. The WPE of the blue LD in our prototype reflective cavity package is 30%, so the corresponding LES is 82 lm/W_e, similar to the LES of nitride white LEDs in early 2010s [2] and superior to other packaged phosphor-converted white lasers. [10,17] If we use state-of-the-art blue LDs with a WPE of 51.2%,[25] the LES in this package would be increased to 143 lm/W_e. Considering that white LED lighting efficacy has doubled in the past decade from 85 lm/W_e to 185 lm/W_e mainly due to the great improvement in blue LED WPE, [2] we believe that the blue LD efficiency will also catch up accordingly. If the blue LD WPE reaches 75% (i.e. similar to blue LEDs or InGaAs infrared LDs[26]) and the interior of the cavity is substituted with DBR reflector to achieve >80% light extraction efficiency, the LES of PC-LD lighting would be increased to ~275 lm/W_e, ~1.5x better than the current LED lighting (185 lm/W_e) and even surpassing the target of LED lighting for 2035 (249 lm/W_e). [2] The optimization of the cavity packaging and selection of high efficiency phosphor are expected to further boost the LES. Hence, the reflective cavity PC-LD lighting prototype demonstrated here can potentially be applied to next-generation high efficacy, high brightness lighting surpassing their LED counterparts.

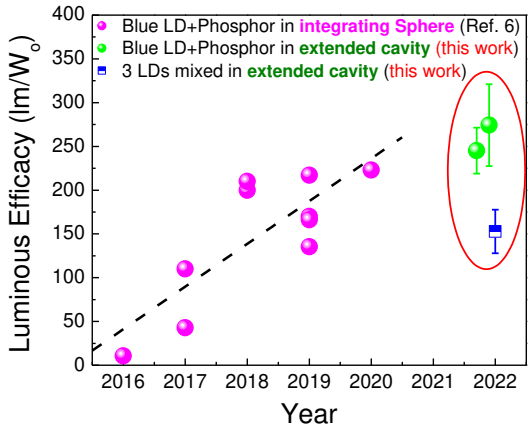

Fig. 8 Luminous efficacy in reference to the input optical power (LEO, lm/W_o) of white LD lighting over time. The dashed line is a linear fit to show the rapid development trend of the PC-LD white lasers over the past decade. The purple data points are from the references in Table 1 of Ref. 6 (a review paper).

Fig. 8 also includes our CM-LD lighting. For color-mixed white light, dichroic mirrors are widely used to combine different colors of lasers,[18,19,20] where the backward scattered light is often wasted, and diffusers are not sufficient to suppress laser speckles. Our CM-LD light sources based on multi-stage color mixing and photon recycling exhibit low speckle contrast, good illumination uniformity, high light extraction efficiency and high luminous efficacy. To our knowledge, it is the first demonstration of a CM-LD light source in a compact package applicable to practical lighting with a high LEO of 150 lm/W_o, comparable to their PC-LD counterparts (Fig. 8). There is still much room to improve the LEO by increasing the packaging efficiency and using high efficiency orange/amber LD for high LER and good color quality. Considering that CM-LEDs are

projected to achieve LES=280 lm/W_e by 2035,[2] it is expected that the corresponding improvement in orange/amber light emitting semiconductors will also enhance the efficiency of CM-LD white lighting beyond 300 lm/W_e, as supported by theoretical optimization of 4-LD lighting. [7]

The laser-based white light can also find applications in VLC simultaneously. In PC-LD configurations, our reflective cavity packaging enables WDM with several blue LDs emitting at slightly different wavelengths (e.g. spaced by a few nm). In CM-LD configurations, each laser source can be modulated separately for data communication. In contrast to existing dichroic mirror color mixing for VLC, which requires elaborate choices of pectral response and optical alignment of the laser beams, our reflective cavity package is much more scalable towards larger numbers of LDs for WDM channels because the color mixing is insensitive to the LD positions, thanks to multiple scattering and reflections. An example of mixing 4 LDs using the reflective cavity package is shown in Section 5 of the Supplemental Information. Modeling shows a high LEO of ~200 lm/W_o using LDs at 450, 520, 630, and 670 nm, while experimentally ~100 lm/W_o has been demonstrated, as has been included in Table 4. The discrepancy is mainly due to the limited power output of commercial 640 nm LD. It can be further improved by substituting the two red LDs with yellow/orange ones. The data rate could also be further improved in the future with the rapid development of high-power, high-speed photonic crystal surface emitting lasers (PCSELs). [27,28]. We will investigate the capability of high data rate with our white laser platform in the future, as well as heat sink design for more effective heat dissipation for multiple LDs.

In conclusion, we demonstrate a universal package for color-mixed white LD and phosphor-converted white LD lighting via multiple-scattering and photon recycling. The impact of the mixing rod, combined diffusers and reflective cavity configuration are systematically investigated in terms of extraction efficiency, irradiace uniformity, augular distribution, speckle contrast, luminous efficacy and color characteristics. After balancing these factors, we demonstrate RGB CM-LD lighting with an extraction efficiency ≥ 60%, CCT of 4500 K, a speckle contrast ≤ 5%, and a luminous efficacy of 150 lm/W_o with respect to the input laser power. To our knowledge, this is the first experimental demonstration of a CM-LD light source in a compact package applicable to practical lighting, with a luminous efficacy comparable to their PC-LD counterparts reported in literature. A simple replacement of the output diffuser with a yellow phosphor plate converts the CM_LD luminaire to a PC-LD lighting package, achieving a luminous efficacy close to 300 lm/W_o and a CRI of ~90. With future improvement of blue laser efficiency and development of amber/orange laser diodes, we envision that this universal reflective cavity white laser package can potentially achieve a luminous efficacy >275 lm/W_e in reference to the input electrical power, ~1.5x higher than state-of-the-art LED lighting and exceeding the target of 249 lm/W_e for 2035.[2] The same white lighting package also offers potentials for synergistic high-speed VLC. These results suggest the dawn of white laser lighting towards practical applications.

Materials and Methods

Modeling of diffusers. The property of diffusers is treated as bulk scattering in ray-tracing simulations based on the micro-particle scattering behavior using TracePro software. [29] Bulk scattering can be modeled by three parameters: the absorption coefficient μ_a, the scattering coefficient μ_s, and the phase function $p(\theta)$. The simple Henyey-Greenstein phase function $p_{HG}(\theta)$ is used, given by Eq. (1)

$$p_{HG}(\theta) = \frac{1-g^2}{4\pi(1+g^2-2g\cos(\theta))^{3/2}} \quad (1)$$

Here g is the anisotropy factor, which is the average cosine of the scattering θ for all the scattering events. The g value varies from -1 to 1. Scattering occurs isotropically at $g = 0$. Light is preferentially forward-scattered for > 0 , and backward-scattered at $g < 0$, respectively. The bulk scattering parameters are μ_a=0 mm^{-1}, μ_s= 35 mm^{-1}, and $g = 0.99$ to describe high efficiency DiffsTEK^{TM} diffusers (D6060 and D3030) [21] used in our experimental studies. More accurate parameters can be determined from the measured transmittance and reflectance with the inverse adding–doubling method.[30]

***Efficiency Definitions*.** Some definitions and relations of luminous efficacies are clarified here. The afore-mentioned LER quantifies the visible light content of the emitted spectrum by comparing the luminous flux (in lumens) to the total radiant output (in Watts): [31]

$$LER = \frac{K_m \int V(\lambda)S(\lambda)d\lambda}{\int S(\lambda)d\lambda} \quad (2),$$

where K_m=683 lm/W, the maximum LER for photopic vision, $S(\lambda)$ is the spectral distribution of the emitted spectrum, and $V(\lambda)$ is the standard luminosity function for photopic vision.

The luminous efficacy of the light source (LES) is the ratio of the output lumen to the input electrical power, as widely used in LED lighting. The unit of LES is lm/W$_e$ in order to distinguish from the luminous efficacy with regard to the input optical power (lm/W$_o$). The latter is named as LEO here, a figure of merit commonly used in the LD lighting community. The relations between LES and LEO for CM-LD lighting and blue-laser excited PC-LD lighting follow Eq.(3) and Eq.(4), respectively.

$$LES(CM) = LEO \times \frac{\sum_{i=1}^{n} P_{i,opt}}{\sum_{i=1}^{n} P_{i,opt}/\eta_{i,wpe}} \quad (3),$$

$$LES(PC) = LEO \times \eta_{b,wpe} \quad (4),$$

where n is the number of discrete laser sources, $P_{i,opt}$ is the optical power of each laser source, and $\eta_{i,wpe}$ is the wall-plug efficiency of each laser source. $\eta_{b,wpe}$ is the wall-plug efficiency of the blue laser used in PC-LD lighting. In general, LEO indicates LD-lighting potential, while LES represents the practical performance depending on the development of the WPE of the LDs.

Another important parameter is the light extraction efficiency η_{ex} of the LD-lighting package, defined as the ratio between the output optical power from the LD lighting package to the input laser power inside the package.[32] It connects LER and LEO in the CM-LD scheme as shown in Eq.(5)

$$LEO = LER \times \eta_{ex} \quad (5)$$

Experimental measurment of specle contrast K_s. A MATLAB program is developed to convert the color image of laser patterns on the letter-sized screen to grayscale in image processing and compute the speckle contrast K_s of the image: [14]

$$K_s = \frac{\sigma_I}{<I>} = \frac{\sqrt{<I^2>-<I>^2}}{<I>} \quad (6),$$

where σ_I is standard deviation of light intensity in the speckle patterns, and $< I >$ is the average intensity.

Experimental measurment of illumination uniformity. To quantify the illumination uniformity, a screen made of letter-sized print paper is placed 30 cm away from the output diffuser towards evaluation of practical lighting. The paper is divided into 48 zones, and the luminous intensity (lux) is measured with a lux meter. The average deviation (AD) is a statistical representation of illumination uniformity, defined as [22]

$$AD = \frac{1}{E_{avg}} \sqrt{\frac{1}{N} \sum_{i=1}^{N} [E(i) - E_{avg}]^2} \quad (7),$$

where N=48 in this case, E_{avg} is the average luminous intensity (lm/m^2, or lux) and $E(i)$ is the luminous intensity measured at the center of the *i* th zone.

Acknowledgments
This project is supported by National Science Foundation, Division of Computer and Network Systems under the award number 2308686. We would like to thank Fusion Optix, Inc. for providing free samples of diffuser sheets used in this study, and Dr. Daniel Scharpf at Labsphere, Inc. for helpful discussions on high-reflectivity white paints.

Author Contributions
X.W. and J.L. conceived the basic idea and design for the reflective cavity white laser mixing. X. Z. conceived the concept of synergy with VLC. X. W. designed and modelled the laser mixing package. C.J.C. made the first version of the prototype and conducted initial testing based on X.W.'s design, which was further improved by X.W. in later versions for more complete experimental characterization. N.R.S and E.R.F provided input and suggestions on the white laser package for future VLC system integration and testing. X.W. wrote the first draft. J.L. revised the manuscript with X.W. based on the input of all the co-authors.

Data availability
All data generated or analyzed during this study are included in this published article (and its Supplemental Information files). The numerical datasets generated during and/or analyzed during the current study are available from the corresponding authors upon reasonable request.

Code availability
The codes developed for this work are available from the authors under reasonable request

Conflict of Interest
The authors declare no competing interest.

Supplemental Information includes specifications of the RGB laser diodes, simulated optical irradiance distribution for a conical reflective cavity, effect of mixing rod length from modeling, a description of the optical components of the laser mixing cavity used in the experiments, and a preliminary demonstration of 4-laser mixing.

REFERENCES

[1] International Energy Agency, https://www.iea.org/energy-system/buildings/lighting#tracking

[2] Pattison, M.; Hansen, M.; Bardsley, N.; Thomson, G. D.; Gordon, K.; Wilkerson, A.; Lee, K.; Nubbe, V.; Donnelly, S. U.S. Department of Energy, 2022 Solid-State Lighting R&D Opportunities, February 2022. https://www.energy.gov/eere/ssl/articles/2022-solid-state-lighting-rd-opportunities

[3] Iveland, J.; Martinelli, L.; Peretti, J.; Speck, J. S.; Weisbuch, C. Direct Measurement of Auger Electrons Emitted from a Semiconductor Light-Emitting Diode under Electrical Injection: Identification of the Dominant Mechanism for Efficiency Droop. *Phys. Rev. Lett.* **2013,** *110*, 177406, DOI: 10.1103/PhysRevLett.110.177406

[4] Lee, C.; Shen, C.; Oubei, H. M.; Cantore, M.; Janjua, B.; Ng, T. K.; Farrell, R. M.; El-Desouki, M. M.; Speck, J. S.; Nakamura, S.; Ooi, B. S.; DenBaars, S. P. 2 Gbit/s data transmission from an unfiltered laser-based phosphor-converted white lighting communication system. *Optics. Express.* **2015,** *23*, 29779-29787, DOI: 10.1364/OE.23.029779

[5] Teschler, L. Energy efficient lighting with laser diodes. Design World, 14 November **2018.** [Online]. Available: https://www.designworldonline.com/energy-efficient-lighting-with-laser-diodes/

[6] Ma, C.; Cao, Y. Phosphor converters for laser driven light sources. *Appl. Phys. Lett.* **2021,** *118*, 210503, DOI: 10.1063/5.0053581

[7] Soltic, S.; Chalmers, A. N. Prospects for 4-laser white-light sources. *J. Mod. Opt.* **2019,** *66,* 271-280, DOI: https://doi.org/10.1080/09500340.2018.1517904

[8] Manabe, Y.; Ishino, M.; Fuji, H.; Kinoshita, H. J.; Fujioka, K.; Yamamoto, K. Improvement of color rendering index of BGYR laser illuminants. *Opt. Rev.* **2022,** *29,* 267-275, DOI: 10.1007/s10043-021-00717-w

[9] Lenef, A.; Kelso, J. F.; Serre, J.; Kulkarni, A. A.; Kinenon, D.; Avison, M. Co-sintered ceramic converter for transmissive laser-activated remote phosphor conversion. *Appl. Phys. Lett.* **2022,** *120,* 021104, DOI: 10.1063/5.0077125

[10] Ma Y.; Luo, X. Packaging for laser-based white lighting: status and perspectives. *J. Electron. Packag.* **2020,** *142*, 010801, DOI: 10.1115/1.4044359

[11] Alingöz, C. Laser technology in automotive lighting. *Proc. SPIE 8965, High-power didode laser technology and applications XII*. **2014,** *896518*, DOI: 10.1117/12.2036519

[12] Neumann, A.; Wierer, J. J.; Davis, W.; Ohno, Y.; Brueck, S. R. J.; Tsao, J. Y. Four-color laser white illuminant demonstrating high color-rendering quality. *Opt. Express* **2011,** *19,* A982, DOI: 10.1364/OE.19.00A982

[13] Deng, L.; Dong, T.; Fang, Y.; Yang, Y.; Gu, C.; Ming, H; Xu, L. Speckle reduction in laser projection based on a rotating ball lens. Opt. Laser Technol. **2021,** *135*, 106686, DOI: 10.1016/j.optlastec.2020.106686

[14] Kumar, V.; Gupta, M; Dubey, A. K.; Tayal, S.; Singh, V.; Mehta, D. S. Design and development of laser speckle reduction device using waveguide diffuser and pyramidal cavity for projection imaging. *J. Opt.* **2020,** *22,* 115601, DOI: 10.1088/2040-8986/abb41b

[15] Ouyang, G.; Tong, Z.; Akram, M. N.; Wang, K.; V. Kartashov, V.; Yan, X.; Chen, X. Speckle reduction using a motionless diffractive optical element. *Opt. Lett.* **2010,** *35*, 2852-2854, DOI: 10.1364/OL.35.002852

[16] Sun, S.-C.; Moreno, I.; Lo, Y.-C.; Chiu, B. C.; Chien, W.-T. Collimating lamp with well color mixing of red/green/blue LEDs. *Opt. Express* **2012,** *20*, A75-A84, DOI: 10.1364/OE.20.000A75

[17] Sun, C. C.; Lin, S.-K.; He, M.-T.; Wu, C.-S.; Yang, T.-H.; Yu, Y. -W. Enhancement of laser multiplexing efficiency for solid state lighting through photon recycling. *IEEE Photon. J.* **2021,** *13*, 1600106, DOI:10.1109/JPHOT.2021.3110944

[18] Huang, Y.-F.; Chi, Y.-C.; Chen, M.-K.; Tsai, D.-P.; Huang, D.-W.; Lin, G.-R. Red/green/blue LD mixed white-light communication at 6500K with divergent diffuser optimization. *Opt. Express* **2018,** *26*, 23397-23410, DOI: 10.1364/OE.26.023397

[19] Chun, H.; Gomez, A.; Quintana, C.; Zhang, W.; Faulkner, G.; O'Brien, D. A wide-area coverage 35 Gb/s visible light communications link for indoor wireless applications. *Sci. Rep.* **2019,** *9*, 4952, DOI: 10.1038/s41598-019-41397-6

[20] Wu, T.-C.; Chi, Y.-C.; Wang, H.-Y.; Tsai, C.-T.; Huang, Y.-F.; Lin, G.-R. Tricolor R/G/B laser diode based eye-safe white lighting communication beyond 8 Gbit/s. Sci. Rep. **2017,** *7*, 11. DOI: 10.1038/s41598-017-00052-8

[21] DiffsTEK™ diffusers in https://www.fusionoptix.com/product/optics/diffusers/

[22] Shadalou, S.; Gurganus, D.; Cassarly, W. J.; Davies, M. A; Suleski, T. J. Design, fabrication, and characterization of a tunable LED-based illuminator using refractive freeform arrays. *Opt. Express* **2022,** *30*, 42749-42761, DOI: 10.1364/OE.474842

[23] Roelandt, S.; Meuret, Y.; Jacobs, A.; Willaert, K.; Janssens, P.; Thienpont, H.; Verschaffelt, G. Human speckle perception threshold for still images from a laser projection system. *Opt. Express* **2014,** *22*, 23965-23979, DOI: 10.1364/OE.22.023965

[24] Ma, Y.; Luo, X. Small-divergent-angle uniform illumination with enhanced luminance of transmissive phosphor-converted white laser diode by secondary optics design. *Opt. Lasers Eng.* **2019,** *122*, 14-22, DOI: 10.1016/j.optlaseng.2019.05.022

[25] Nakatsu, Y.; Nagao, Y.; Hirano, T.; Kozuru, K.; Kanazawa, T.; Masui, S.; Okahisa, E.; Yanamoto, T.; Nagahama, S. "Edge-emitting blue laser diode with high CW wall-plug efficiency of 50%", *Proc. SPIE* **2022**, *12001*, 1200109. DOI: 10.1117/12.2601154

[26] Piprek, J. What Limits the Efficiency of High-Power InGaN/GaN Lasers? *IEEE. J. Quant. Electron.* **2017**, 53, 2000104

[27] Q. Liu, Z. Wang, X. Ma, J. Wang and W. Zhou, "Design of GaN-Based PCSEL With Temperature-Insensitive Lasing Wavelength," in *IEEE Photonics Journal*, vol. 13, no. 4, pp. 1-6, Aug. 2021, Art no. 1500306, doi: 10.1109/JPHOT.2021.3091140.

[28] T. Inoue, M. Yoshida, M. D. Zoysa, K. Ishizaki, and S. Noda, "Design of photonic-crystal surface-emitting lasers with enhanced in-plane optical feedback for high-speed operation," Opt. Express 28, 5050-5057 (2020)

[29] TracePro 7.0 User Manual, https://lambdares.com/

[30] Leyre, S.; Leloup, F. B.; Audenaert, J.; Durinck, G.; Hofkens, J.; Deconinck, J. G.; Hanselaer, P. Determination of the bulk scattering parameters of diffusing materials. *Appl. Opt*. **2013,** *52*, 4083-4090, DOI: 10.1364/AO.52.004083

[31] Wyszecki, G.; Stiles, W. S. *Color Science: Concepts and Methods, Quantitative Data and Formulae, 2nd ed*.; Wiley: New York, 1982.

[32] Sun, C. C.; Chang, Y. Y.; Yang, T. H.; Chuang, T. -Y.; Chen, C.-C.; Lee, T.-X.; Li, D.-R.; Lu, C.-Y.; Z.-Y. Ting, Z.-Y.; Glorieux, B.; Chen, Y.-C.; Lai, K.-Y.; Liu, C.-Y. Packaging efficiency in phosphor-converted white LEDs and its impact to the limit of luminous efficacy. *J Sol. State Light* **2014,** *1*, 19, DOI: 10.1186/s40539-014-0019-0

Supplementary Files

This is a list of supplementary files associated with this preprint. Click to download.

- SupplementaInformation7182023LSASubmissionClean.docx